Proc. Natl. Acad. Sci. USA
Vol. 81, pp. 4790–4794, August 1984
Biophysics

Fluorescence quantum yield of visual pigments: Evidence for subpicosecond isomerization rates

(primary event/*cis–trans* isomerization/excited-state potential surfaces/barrier-less rotation)

A. G. DOUKAS*, M. R. JUNNARKAR*, R. R. ALFANO*, R. H. CALLENDER*, TOSHIAKI KAKITANI†‡, AND BARRY HONIG†

*Physics Department, The City College of The City University of New York, New York, NY 10031; and †Department of Biochemistry, Columbia University, 630 West 168 Street, New York, NY 10032

Communicated by Melvin Lax, March 5, 1984

ABSTRACT The fluorescence quantum yields (ϕ_f) for bovine and squid rhodopsins are determined. Both pigments yield similar results, with an average value for ϕ_f of 1.2 (±0.5) $\times 10^{-5}$. Since the estimated radiative lifetime of rhodopsin is 5 nsec, the rate constant of the process that competes with fluorescence must be on the order of 0.1 psec. Given the large quantum yield for isomerization of rhodopsin's retinal chromophore, this process is likely to correspond to the motion along retinal's C11-C12 torsional coordinate that leads to *cis–trans* isomerization. An empirical excited-state potential energy curve along this coordinate is derived. It is shown that subpicosecond torsional motion to highly twisted nonfluorescing regions of the potential is possible and, in fact, likely. Our results require the existence of a barrier-less excited-state potential energy curve and suggest that *cis–trans* isomerization occurs in <1 psec.

Visual pigments consist of a single chromophore, 11-*cis* retinal, covalently bound in the form of a protonated Schiff base to the ε-amino group of lysine-321 in the apoprotein opsin (for a recent review, see ref. 1). The visual process is initiated by a photochemical event in which rhodopsin is transformed into its primary photoproduct, bathorhodopsin. It has been well-established that the rhodopsin to bathorhodopsin transition is driven by an 11-*cis* to all-*trans* photoisomerization of the *in situ* retinal chromophore. Given the central importance of this process, great efforts have been invested in its detailed characterization.

The potential energy curve along the C11-C12 torsional coordinate that connects the rhodopsin and bathorhodopsin ground states can be described with considerable accuracy (2, 3). There is an unusually large enthalpy increase, the value of which has been determined by Cooper to be 35 kcal/mol (1 cal = 4.184 J) (3). Based on this value and the absence of a thermal back-reaction at 77 K, a lower limit for the activation energy of 42 kcal/mol can be established (see below). As we discuss below, the upper limit is at most a few kcal/mol higher than this value. The unusual shape of the ground-state potential is due to specific protein–chromophore interactions designed to enhance the stability of rhodopsin to thermal isomerization and to produce the high energy photoproduct bathorhodopsin (2).

The excited-state potential energy surface is clearly designed to facilitate an efficient 11-*cis* to all-*trans* photoisomerization (2). The quantum yield for the process is, indeed, unusually high (0.67), and this value remains constant at temperatures as low as 77 K (4). Moreover, the primary event is extremely fast, occurring on picosecond, or perhaps subpicosecond, time scales (5–8). In light of the fact that protonated Schiff bases in solution do not exhibit such unusual photolability (9), it is of interest to determine how the properties of the chromophore are so drastically altered on binding to the protein. Based on an analysis of the photochemistry, it was proposed that rhodopsin and bathorhodopsin are connected by an excited-state potential with a single minimum along the C11-C12 torsional coordinate (4, 10). Extended quantum mechanical calculations can indeed produce a potential of this type (for a review, see ref. 11); however, there has been no experimental evidence as to the actual shape of the curve. Once this is determined it may be possible to construct models for the protein–chromophore interactions that lead to the observed potential.

Fluorescence from rhodopsin has been difficult to observe because of its apparently low quantum yield and the presence of sample impurities. Recently, however, the rise and decay times of the fluorescence of bovine rhodopsin were measured and found to be <12 psec at room temperature (12). In this paper, we report the quantum yield of fluorescence for squid and bovine rhodopsin. The yields are so small ($\approx 1.2 \times 10^{-5}$) that they require the existence of an extremely rapid decay mode that competes with emission. Given the high quantum yield for photoisomerization, this mode almost certainly involves torsional motion about the C11-C12 double bond. In the discussion, we show that our results require a barrier-less excited-state potential along this coordinate. Finally, although our measurements detect only the earliest part of the process, our results suggest that photoisomerization may occur in times as short as a few tenths of a picosecond.

METHODS AND MATERIALS

The apparatus used in the fluorescence kinetics measurements has been described (13, 14). A single pulse (1054 nm) from the output of a mode-locked Nd/glass laser was selected and amplified. The second harmonic at 527 nm was used to excite the sample. The exciting beam was collimated to a spot of 1.5×10^{-2} cm^2 and of average density of 8×10^{15} to 1.6×10^{16} photons/cm^2. The energy of the pulse was measured using a Hamamatsu photodiode. The samples were frontally excited and the fluorescence was collected and focused onto a 50-μm entrance slit of a Hamamatsu streak camera. Two 530-nm cutoff filters (3-67 Corning) were placed in the path of the fluorescence to eliminate any scattered laser beam. The Hamamatsu camera was coupled to a GBC video camera. The data were acquired by a Hamamatsu temporal analyzer and were processed in a DEC Minc minicomputer. The fluorescence curves were corrected for time and intensity nonlinearities. The time resolution (FWHM) of the laser-streak camera system was about 15 psec. In some of the measurements, various filters were placed in the fluorescence path to obtain a rough measure of

The publication costs of this article were defrayed in part by page charge payment. This article must therefore be hereby marked "*advertisement*" in accordance with 18 U.S.C. §1734 solely to indicate this fact.

‡Permanent address: Department of Physics, Nagoya University, Nagoya 464, Japan.

the emission spectral profile. The following filters were used: the step function R64, R66, and R68 filters (Hoya Optics, Fremont, CA) and the 2-62 filter (Corning), which pass high wavelengths and whose half-maximum transmissions lie at 640, 660, 680, and 620 nm, respectively; the step function SPF 620 (Ditric Optics, Hudson, MA) filter, which passes short wavelength radiation and whose half-maximum transmission lies at 620 nm; and a narrow band pass filter (which we call NBF 620) whose maximum transmission is at 620 nm with a FWHM of 10 nm.

Squid rhodopsin (Todarodes Pacificus), a gift from Tatsuo Suzuki, was prepared by the method of Suzuki *et al.* (15). The sample was treated with hydroxylamine and then passed through Sephadex G-100, resulting in a solution free from retinochrome. Squid rhodopsin was solubilized in 0.2% digitonin and 0.2 M NaCl. Bovine rhodopsin was prepared by the method of Papermaster and Dryer (16). The A_{280}/A_{500} absorbance ratio was found to be ≈2.5. The rhodopsin outer segments were suspended in 0.067 M potassium buffer (pH 6.8), and 0.1 M hydroxylamine was added to reduce any free retinal arising from the photolysis of rhodopsin.

The fluorescence of rhodopsin was compared to the known fluorescence quantum yield (17) of erythrosin (Eastman Kodak: erythrosin disodium salt, P110) in water. The fluorescence measurements of rhodopsin and erythrosin were taken under identical conditions of scattering geometry, diameter of exciting beam, slit width, microchannel plate gain, and sweep speed.

A 2-mm cuvette was connected to a piston pump and reservoir containing ≈15 ml of sample. The sample was circulated to replenish photolyzed rhodopsin. A 2-mm cuvette was used for erythrosin. All measurements were taken at room temperature. The optical density of the solubilized squid rhodopsin was 1.2 at 527 nm. The optical density of bovine rhodopsin was 0.56 at 527 nm. The bovine outer segments, however, also showed a high scattering of ≈1.4 OD, because the samples were not solubilized.

RESULTS

Fig. 1 *a* and *b* shows typical fluorescence kinetics (integrated from 560 to 800 nm) from squid rhodopsin and alkaline metarhodopsin, respectively. The metarhodopsin species was formed by a lamp irradiating the rhodopsin sample at pH 10.5 at room temperature. This converted squid rhodopsin (absorption maximum, 485 nm) to alkaline metarhodopsin (absorption maximum, 380 nm). Fig. 1*a* can be fitted to a biexponential with a "fast" component, which is resolution limited, and a "slow" component with a lifetime of ≈200 psec. The fast component disappears in the data of Fig. 1*b*, leaving only the slow component. In a previous study of bovine rhodopsin (12), a similar unresolved fast and resolved slow component was observed, the former disappearing when the sample was bleached in the presence of hydroxylamine. The slow component would appear to arise from some fluorescing center (possibly impurities) not associated with rhodopsin chromophore. The fact that the fast component disappears on "bleaching" suggests that it arises from the chromophore of rhodopsin. Furthermore, the determined quantum yields of both squid and bovine rhodopsins (see below), based on the fast component, are the same within our signal-to-noise ratio. This observation also strongly implies that the fast fluorescence component is due to the intrinsic chromophore. The final decisive proof could be provided by an action spectrum of the fast component, but this experiment is not possible with our present equipment. In what follows, we make the operating assumption that the unresolved fluorescence is due to the chromophore of rhodopsin and not from some other source. At the very least, our results provide an upper limit to the fluorescence quantum yield.

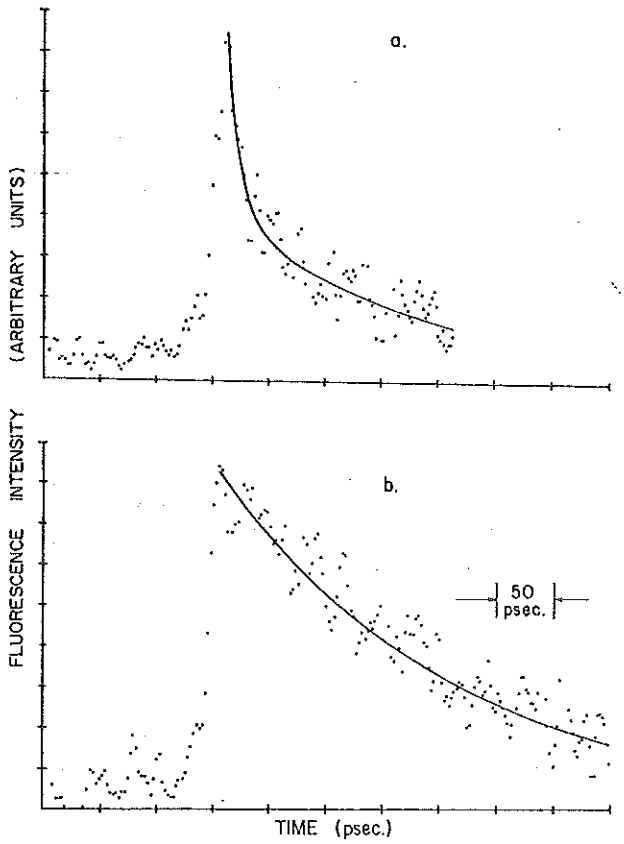

FIG. 1. Typical fluorescence kinetics integrated from 560 to 800 nm of squid rhodopsin (*a*) and squid alkaline metarhodopsin (*b*) excited by a 527-nm pulse.

We obtain the integrated intensity of the fast component by extrapolating the intensity kinetics of the slow component to zero time and subtract this from the observed fluorescence of Fig. 1*a*. A series of cut-off filters were used to obtain the emission profile. By suitably subtracting the observed emission intensity from one filter by another, the emission within a wavelength window can be obtained. The squid emission spectra for both the slow and fast components are given in Fig. 2. The horizontal bars represent the window half-width (FWHM). As can be seen, the fast emission peaks at ≈620 nm.

The fluorescence of erythrosin at 1 mM concentration was also taken under identical conditions. The relative quantum yield of rhodopsin is given by

$$\phi_f^R = \frac{I_R}{I_E}\frac{N_E}{N_R}\phi_f^E$$

where ϕ_f^E is the quantum yield of erythrosin (0.02), and I_R and I_E are the time-integrated intensities of the fluorescence of rhodopsin and erythrosin, respectively. The integrated intensities are normalized for the intensity of the exciting pulse, the gain of the temporal analyzer, the spectral response of the streak camera, and, in the case of the erythrosin, for the neutral density and the two 530-nm cutoff filters in front of the camera. N_E and N_R are the percentage of photons absorbed by erythrosin and rhodopsin samples, respectively.

Bovine rhodopsin was measured under the same conditions. Fig. 3 *a* and *b* shows typical data on the integrated fluorescence emission (from 560 to 800 nm) of rhodopsin and bleached rhodopsin, respectively. The rhodopsin samples used here show a greatly reduced slow-emission component relative to that previously reported. Here we observe pri-

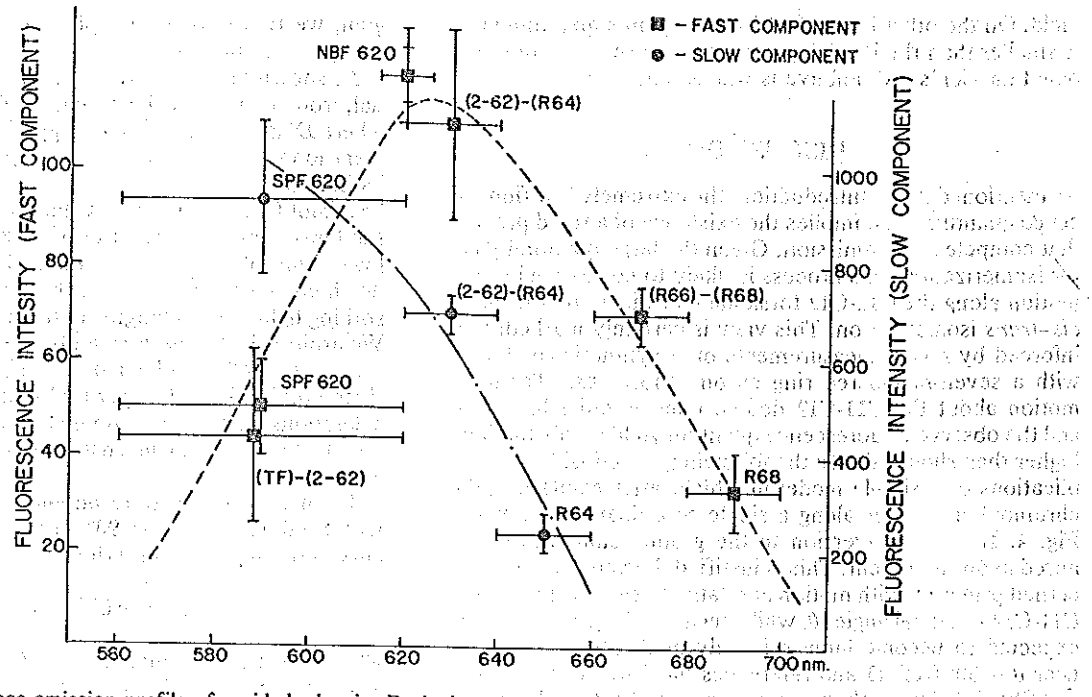

FIG. 2. Fluorescence emission profile of squid rhodopsin. Dashed curve, fast component; dot-dashed curve, slow component. TF, total integrated fluorescence.

marily the unresolved fast emission (Fig. 3*a*), which disappears in bleached samples (Fig. 3*b*). This confirms our previous assignment (12) of the slow component as arising from fluorescing centers not associated with rhodopsin's active site, because the intensity of the slow component clearly changes with sample preparation. Within our signal-to-noise ratio, the emission characteristics of the fast component are the same as those found for the squid pigment except that the emission peak is shifted to ≈600 nm. The error in determining the emission peak is about ±15 nm for both pigments.

Two separate samples were measured for both of the squid and bovine pigments. Using $\phi_f^B = 0.02$, we found an average $\phi_f^R = 0.9\ (\pm 0.5) \times 10^{-5}$ and $1.4\ (\pm 0.4) \times 10^{-5}$ for the squid pigment and $\phi_f^R = 1.3\ (\pm 0.6) \times 10^{-5}$ and $1.3\ (\pm 0.4) \times 10^{-5}$ for the bovine pigment.§ Each run of the four samples consisted of 10–15 actinic pulses, and the error is the standard deviation of the individual runs. In the discussion below, we use the average value of $\phi_f = 1.2\ (\pm 0.5) \times 10^{-5}$ as the quantum yield of rhodopsin.

In our measurements, a possible source of systematic error can arise from the photochemistry of rhodopsin. It is well known that rhodopsin is first photoconverted to bathorhodopsin and then to isorhodopsin. Both these pigments can absorb subsequent photons and could contribute to the observed fluorescence, depending on their concentration and on fluorescence quantum yields. To examine this possibility, a mathematical analysis of the photochemistry, using known absorption cross-sections, photochemical quantum yields, and our light power densities was undertaken to quantify the amount of bathorhodopsin and isorhodopsin formed during the actinic pulse. We found that the average amount of these species present during the pulse was 6% bathorhodopsin and 3% isorhodopsin in the squid experiments and 30% bathorhodopsin and 6% isorhodopsin in the bovine experiments. These numbers introduce errors that are within our standard deviations, and the fluorescence quantum yields given above have not been modified on their account. Furthermore, it is unclear what corrections to make. Our previous results (12) showed that the fluorescence quantum yield from isorhodopsin is similar to that of rhodopsin so that any correction would simply scale with isorhodopsin's concentration, an insignificant correction compared to other uncertainties. However, we do not know the fluorescence characteristics of bathorhodopsin at this time. If bathorhodopsin's quantum yield were 10–20 times larger than rhodopsin's, the observed fluorescence would be dominated by this pigment, and our results would be an upper limit to rhodopsin's quantum

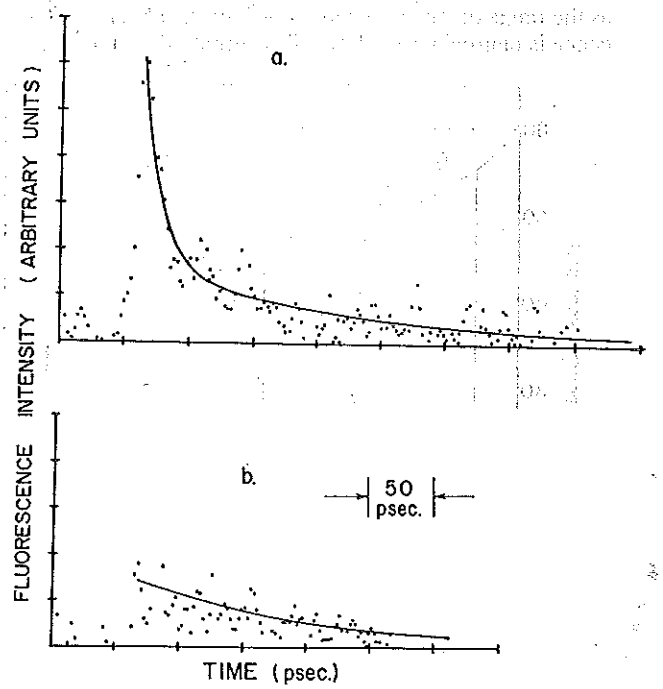

FIG. 3. Typical fluorescence kinetics integrated from 560 to 800 nm of bovine rhodopsin (*a*) and bleached bovine rhodopsin (*b*) excited by a 527-nm pulse.

§Using other methodologies, R. R. Birge, J. A. Bennett, and L. P. Murray (personal communication) found a quantum yield for bovine rhodopsin of $7.8\ (\pm 2.3) \times 10^{-6}$, a result in good agreement with ours.

yield. On the other hand, if bathorhodopsin's quantum yield is smaller than rhodopsin's, a small increase in the reported quantum yields given above is warranted.

DISCUSSION

As mentioned in the Introduction, the extremely low fluorescence quantum yield implies the existence of a rapid process that competes with emission. Given the large quantum yield for isomerization, this process is likely to correspond to the motion along the C11-C12 torsional coordinate that leads to *cis–trans* isomerization. This view is certainly markedly reinforced by recent measurements on a synthetic rhodopsin with a seven-membered ring chromophore (18). Torsional motion about the C11-C12 double bond is quite hindered, and the observed fluorescence quantum yield is substantially higher than rhodopsin. In the following, we consider the implications of a simple model in which, after excitation, the chromophore moves along a single coordinate as shown in Fig. 4. Internal conversion to the ground state will be ignored in our treatment. This is justified, because we are concerned primarily with motion at relatively small values of the C11-C12 torsional angle, θ, while decay to the ground state is expected to become large primarily in the crossing region near $\theta = 90°$ (ref. 11 and references therein). In fact, Dinur and Sharf (19) have shown in a recent publication that internal conversion in the planar configuration of rhodopsin should be extremely slow.

It is useful to define a radiative lifetime, $\tau_r(\theta)$, which varies as a function of torsional angle. $\tau_r(0)$ has been estimated from the integrated area under the absorption band to be 5 nsec (12). As the molecule moves along the excited-state surface, $\tau_r(\theta)$ varies due primarily to the ν^{-3} dependence of the Einstein coefficient for spontaneous emission. [Calculations indicate that the transition dipole is not affected significantly by changes in θ, in agreement with the Condon approximation (unpublished results).] Since the transition energy decreases dramatically as θ increases (from ≈50 kcal/mol at 0° to near 0 kcal/mol at $\theta = 90°$), $\tau_r(\theta)$ should increase over many orders of magnitude. We define the fluorescing region as the range of θ over which "most" of the observed fluorescence is emitted (see below). To estimate the fluorescing region, we first derive a simple expression for the transition energy as a function of θ.

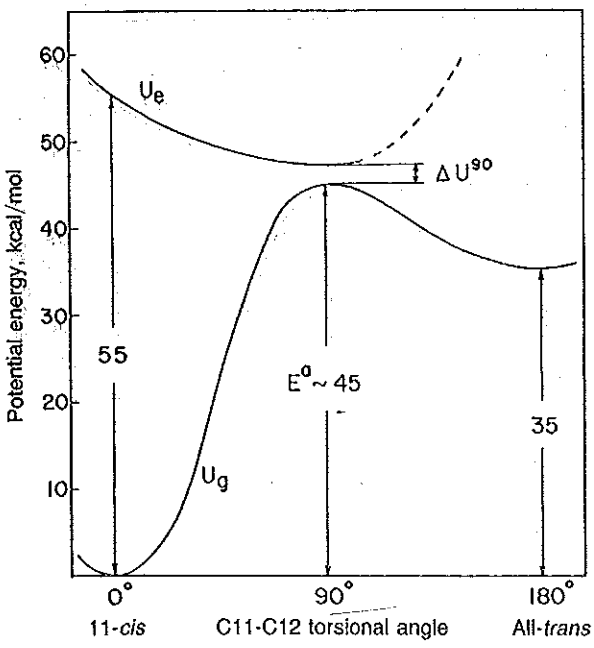

FIG. 4. A scheme of the ground- and excited-state potential surfaces along the chromophore C11-C12 torsional coordinate.

As shown in Fig. 4, we represent the ground-state potential, from 0° to 90°, with a function of the form $U_g = E^a \sin^2\theta$, where E^a is the activation energy. For the chicken cone pigment iodopsin, the activation energy for the back-reaction, bathorhodopsin to iodopsin, has been estimated to be >7 kcal/mol (20). Adding this value to the rhodopsin to bathorhodopsin enthalpy increase of 35 kcal/mol, we arrive at a lower limit of $E^a = 42$ kcal/mol. The upper limit cannot be much greater than this value, because rhodopsin begins absorbing light at wavelengths corresponding to ≈48 kcal/mol. We arbitrarily choose a mean between these two values and assume that $E^a = 45$ kcal/mol. A similar value has been derived previously by Cooper (3) based on closely related considerations. It should be pointed out that the conclusions of our analysis are quite insensitive to the exact value of E^a that is used.

To fit the excited-state potential, we assume a parabola with a minimum at $\theta = 90°$. If we assume that there is no curve crossing, we can write

$$U_e = E^a + \Delta U^{90} + (k^e/2)(\theta - 90)^2 \quad [1]$$

where k^e is a force constant and ΔU^{90} is the vertical distance at $\theta = 90°$ between the top of the ground-state potential and the bottom of the excited-state potential (see Fig. 4).

Now the excitation energy, ΔU, is just $U_e - U_g$. If, for simplicity, we assume that the two curves just touch at 90°, then $\Delta U^{90} = 0$ and

$$\Delta U(\theta) = (k^e/2)(\theta - 90)^2 + E^a \cos^2\theta. \quad [2]$$

Since ΔU (0°) = 55 kcal/mol and $E^a = 45$ kcal/mol, k^e is found, for this set of values, to be 0.0025 kcal/mol·deg^{-2}. For purposes of the discussion below, we point out that the transition energy decreases to 25 kcal/mol at $\theta = 45°$, so that the ν^3 term in the Einstein coefficient results in τ_r^{-1} (45°) ≈ 0.1 τ_r^{-1} (0°). Similarly, τ_r^{-1} (60°) ≈ 0.01 τ_r^{-1} (0°). It is apparent that almost all of the fluorescence is emitted before the molecule reaches 45°, and we thus define the fluorescing region as $0° < \theta < 45°$. This is somewhat arbitrary, but the qualitative analysis presented here is quite insensitive to the actual values we use.

The molecule must rotate out of the fluorescing region in a time, τ_f, which is an "effective" fluorescent lifetime. This is related to the quantum yield, ϕ_f. However, the usual expression $\phi_f = \tau_f/\tau_r$, is not valid in this case, because τ_r is now a variable. It is necessary to perform a time-dependent integration of τ_r over all values of θ to obtain a correct expression for the quantum yield (unpublished data). Here we simply assume an average value of $\tau_r(\theta)$, which we take to correspond to τ_r (22.5°)—i.e., the radiative lifetime in the middle of the fluorescing region. This is found to be 10 nsec. Averaging our values of ϕ_f for both squid and bovine rhodopsin, we find $\phi_f = 1.2\ (\pm 0.5) \times 10^{-5}$ and thus, $\tau_f = 1.2\ (\pm 0.5) \times 10^{-13}$ sec. Our results thus imply that the chromophore rotates out of the fluorescing region (from 0° to 45°) in ≈0.12 psec.

This is a very short time, and it is important to ask whether such a rapid motion is consistent with the constraints we have placed on the potential functions. Assuming a rigid body rotation of the Schiff base terminus of the retinal molecule plus two carbons in the lysine side chain, a moment of inertia of $I = 250\ m_p \cdot Å^2$ may be estimated where m_p is the mass of a proton. Since, depending on the actual motion, the true moment of inertia may be much smaller than this value, we will consider I as a parameter and determine τ_f for values of $I = 250$, 100, and 25. Since the period of oscillation in the excited-state parabola is given by $T_e = 2\pi(I/k)^{1/2}$ (where the

Table 1. Calculated and experimental fluorescence lifetimes (psec)

	$I = 250$	$I = 100$	$I = 25$
τ_f (for $\Delta U^{90} = 0$ kcal/mol)	0.28	0.17	0.08
τ_f (for $\Delta U^{90} = 7.5$)	0.56	0.34	0.16

$\tau_{experiment} = 0.12 \pm 0.05$ psec.

force constant is expressed in radians), we find $T_c = 1.7 \times 10^{-12}$ sec for $I = 250$, 1.0×10^{-12} sec for $I = 100$, and 0.5×10^{-12} sec for $I = 25$.

Now the equation of motion along the excited-state parabola is given by

$$\left(\frac{\pi}{2} - \theta\right) = \left(\frac{\pi}{2}\right)\cos(2\pi t/T_c). \qquad [3]$$

When $\theta = 45°$, t corresponds to the time the excited-state molecule spends in the fluorescencing region, τ_f. By substituting T_c into Eq. 3, we arrive at the values for τ_f summarized in Table 1 (for the case $\Delta U^{90} = 0$). It is clear that, even assuming a rigid body moment of inertia ($I = 250$), an extremely rapid torsional motion is obtained. However, the value of τ_f for this case is outside the experimentally defined range. For $I = 100$, the calculated τ_f corresponds to the experimentally defined upper limit, while $I = 25$ is close to the lower limit. It is difficult to know what value of I is actually appropriate. For an isomerization in the gas phase, the rigid body value is clearly too large, and values as small as $I = 25$ may be more realistic (unpublished observations). On the other hand, isomerization in the protein may require that residues, in addition to the lysine, be displaced; and this, of course, would increase the effective moment of inertia.

The experimental uncertainties as well as the uncertainties in the moment of inertia make it difficult to place severe constraints on the shape of the excited-state potential. For example, decreasing the well-depth from, say, 10 to 2.5 kcal/mol would increase τ_f only by a factor of 2 (see Table 1 for the case $\Delta U^{90} = 7.5$). The calculated lifetimes are too large for $I = 250$ and $I = 100$, but $I = 25$ still satisfies the experimental condition.

According to our excited state potential function, the molecule reaches the region of $\theta = 90°$ in a time given by $T_c/4$, or in 0.1–0.5 psec, depending on the value of I. Although our results only measure the beginning of the isomerization process, they do suggest that subpicosecond isomerization times are possible and even likely. This was first demonstrated by Warshel (21) who reported a classical trajectory simulation using his "bicycle pedal" model for visual pigments. More recently Birge and co-workers (22, 23) have carried out extensive simulation studies on the isomerization dynamics of rhodopsin. Our own analysis, while far less sophisticated, has the advantage of both simplicity and the absence of any detailed assumption as to the exact nature of the motion along the excited-state surface. By relating the fluorescence quantum yield to two essential parameters, the slope of the potential in the Franck–Condon region and the moment of inertia, we are able to place constraints on specific models for the photoisomerization mechanism in visual pigments. More accurate experiments as well as studies on various artificial pigments should allow us to further characterize the process.

The low fluorescence quantum yield for rhodopsin suggests that the motion along this torsional coordinate is unusually fast. It is remarkable that the protein matrix allows and even facilitates a significant displacement of atoms in such a short time. There are few precedents for such rapid isomerization rates in model systems, although direct subpicosecond measurements have detected a 0.32 psec isomerization rate for *cis*-stilbene in the vapor phase (24).

We thank Mr. D. Chandra and Dr. J. Buchert for assistance in performing the experiments. This work was supported in part by grants from The National Institutes of Health (EY02515 to City College and GM 30519 to Columbia University) and The National Science Foundation (PCM82-07145 to Columbia University).

1. Ottolenghi, M. (1980) *Adv. Photochem.* 12, 97–200.
2. Honig, B., Ebrey, T. G., Callender, R. H., Dinur, U. & Ottolenghi, M. (1979) *Proc. Natl. Acad. Sci. USA* 76, 2503–2507.
3. Cooper, A. (1979) *Nature (London)* 282, 531–533.
4. Hurley, J. B., Ebrey, T. G., Honig, B. & Ottolenghi, M. (1977) *Nature (London)* 270, 540–542.
5. Busch, G., Applebury, M., Lamola, A. & Rentzepis, P. (1972) *Proc. Natl. Acad. Sci. USA* 69, 2802–2805.
6. Green, B., Monger, T., Alfano, R., Aton, B. & Callender, R. H. (1977) *Nature (London)* 264, 179–180.
7. Peters, K., Applebury, M. & Rentzepis, P. (1977) *Proc. Natl. Acad. Sci. USA* 74, 3119–3123.
8. Monger, T. G., Alfano, R. R. & Callender, R. H. (1979) *Biophys. J.* 27, 105–116.
9. Huppert, D., Rentzepis, P. M. & Kliger, D. S. (1977) *Photochem. Photobiol.* 25, 193–197.
10. Rosenfeld, T., Honig, B., Ottolenghi, M., Hurley, J. & Ebrey, T. G. (1977) *Pure Appl. Chem.* 49, 341–351.
11. Birge, R. R. (1981) *Annu. Rev. Biophys. Bioeng.* 10, 315–354.
12. Doukas, A. G., Lu, P. Y. & Alfano, R. R. (1981) *Biophys. J.* 35, 547–550.
13. Yu, W., Pellegrino, F., Grant, M. & Alfano, R. R. (1977) *J. Chem. Phys.* 67, 1766–1773.
14. Schiller, N. H. & Alfano, R. R. (1980) *Opt. Commun.* 35, 451–454.
15. Suzuki, T., Uji, K. & Kito, V. (1976) *Biochim. Biophys. Acta* 428, 321–338.
16. Papermaster, D. S. & Dryer, W. J. (1973) *Biochemistry* 13, 2438–2444.
17. Bowers, P. G. & Porter, F. R. S. (1967) *Proc. R. Soc. London Ser. A* 299, 348–353.
18. Buchert, J., Stefancic, V., Doukas, A. G., Alfano, R. R., Callender, R. H., Pande, J., Akita, H., Balogh-Nair, V. & Nakanishi, K. (1983) *Biophys. J.* 43, 279–283.
19. Dinur, U. & Sharf, B. (1983) *J. Chem. Phys.* 79, 2600–2608.
20. Hubbard, R., Bownds, D. & Yoshizawa, T. (1965) *Cold Spring Harbor Symp. Quant. Biol.* 30, 301–316.
21. Warshel, A. (1976) *Nature (London)* 260, 679–683.
22. Birge, R. R. & Hubbard, L. M. (1980) *J. Am. Chem. Soc.* 102, 2195–2205.
23. Birge, R. R. & Hubbard, L. M. (1981) *Biophys. J.* 34, 517–534.
24. Greene, B. I. & Farrow, R. C. (1983) *J. Chem. Phys.* 78, 3336–3338.